Acta Oceanol. Sin., 2018, Vol. 37, No. 2, P. 25–34
DOI: 10.1007/s13131-017-1126-8
http://www.hyxb.org.cn
E-mail: hyxbe@263.net

Diagenetic fluids evolution of Oligocene Huagang Formation sandstone reservoir in the south of Xihu Sag, the East China Sea Shelf Basin: constraints from petrology, mineralogy, and isotope geochemistry

HAO Lewei[1*], WANG Qi[1], GUO Ruiliang[1, 2], TUO Chengrong[1, 2], MA Dongxu[1, 2], MOU Weiwei[1, 2], TIAN Bing[1]

[1] Key Laboratory of Petroleum Resources, Gansu Province/Key Laboratory of Petroleum Resources Research, Institute of Geology and Geophysics, Chinese Academy of Sciences, Lanzhou 730000, China

[2] University of Chinese Academy of Sciences, Beijing 100049, China

Received 31 May 2017; accepted 6 July 2017

Abstract

The Oligocene Huagang Formation is the main sandstone reservoir in the Xihu Sag, situated in the east of the East China Sea Shelf Basin. With an integrated approach of thin-section petrography, ultra-violet fluorescence microscopy, scanning electron microscopy, and isotope geochemistry, the different diagenetic features were identified, the typical diagenetic parasequences were established, and the diagenetic fluids evolution history were reconstructed for the Oligocene Huagang Formation sandstone reservoir in the south of Xihu Sag. The Huagang Formation sandstone reservoir is now in Period B of the mesodiagenesis, which has undergone significant diagenetic alterations such as mechanical compaction, Pore-lining chlorite cement, feldspar dissolution, quartz cementation and dissolution, and carbonate cementation. Three types of carbonate cements (early siderite, medium ferrocalcite and late ankerite) were identified in the Huagang Formation sandstone reservoir. The carbon and oxygen isotopic compositions of carbonate cements show that the early calcite precipitate from alkaline lacustrine environment whereas the late carbonate cements were closely related to the organic acids. To the Huagang Formation sandstone reservoir, it has experienced two main episodes of dissolution during diagenesis. The early dissolution is that unstable components such as feldspar, lithic fragments, and carbonate cement were dissolved by acidic water. The second dissolution is that quartz and other silicate minerals were dissolved under the alkaline condition. Two main phases of hydrocarbon charging occurred in this study area. The first hydrocarbon emplacement was prior to the medium carbonate cementation but posterior to feldspar dissolution and the onset of quartz cementation at the end of the Miocene. The second hydrocarbon charging occurred in the Quaternary period after the late carbonate precipitation.

Key words: diagenesis, fluid evolution, Huagang Formation, Xihu Sag

Citation: Hao Lewei, Wang Qi, Guo Ruiliang, Tuo Chengrong, Ma Dongxu, Mou Weiwei, Tian Bing. 2018. Diagenetic fluids evolution of Oligocene Huagang Formation sandstone reservoir in the south of Xihu Sag, the East China Sea Shelf Basin: constraints from petrology, mineralogy, and isotope geochemistry. Acta Oceanologica Sinica, 37(2): 25–34, doi: 10.1007/s13131-017-1126-8

1 Introduction

Reservoir quality is considered as the primary factor in hydrocarbon exploration and production. Many success hydrocarbon explorations depend in large part on discovering sandstone reservoir with sufficient porosity and permeability to support commercial development (Taylor et al., 2010). Generally, porosity and permeability are mainly controlled by the depositional environment and diagenesis. Many factors including physical and chemical factors such as pressure, temperature, fluid property, and the open or closed of the system, influence the pore evolution (Hunt, 1990; Mu and Zhang, 1994; Wilkinson et al., 1997; Osborne and Swarbrick, 1999). Among these factors, the fluid properties play a key role in dissolution and precipitation of minerals (Qiu and Jiang, 2006). Petrography and geochemistry of the infilling cements can provide information on the material transfer mechanisms as well as the fluid types that formed the cements and, hence, paleofluid flow (Wang et al., 2007, 2010; Gier et al., 2008; Zhang et al., 2012; Stroker et al., 2013). Therefore, it is powerful and helps to better understand the changes of the petrophysical properties in reservoir through time by analyzing the petrography and geochemistry on diagenetic cements.

The East China Sea Shelf Basin is a Cenozoic continental margin basin bounded to the west by the Zhemin Uplift, and to the east by the Diaoyudao Uplift Belt (Hsu et al., 2001) (Fig. 1). It contains thick sedimentary fills and abundant oil and gas resource. The Xihu Sag, located in the east of East China Sea Shelf Basin (Fig. 1), is believed to be highly prospective for oil and gas. Several sets of potential sandstone reservoirs have been determined in the Xihu Sag. Among these reservoirs, the Oligocene Huagang Formation, with extensive distribution and large thickness, was

Foundation item: The National Natural Science Foundation under contract Nos 41502142 and 41502110; the National Science and Technology Major Project under contract No.2016ZX05026-007-05; the Youth Innovation Promotion Association CAS.
*Corresponding author, E-mail: haolewei66@163.com

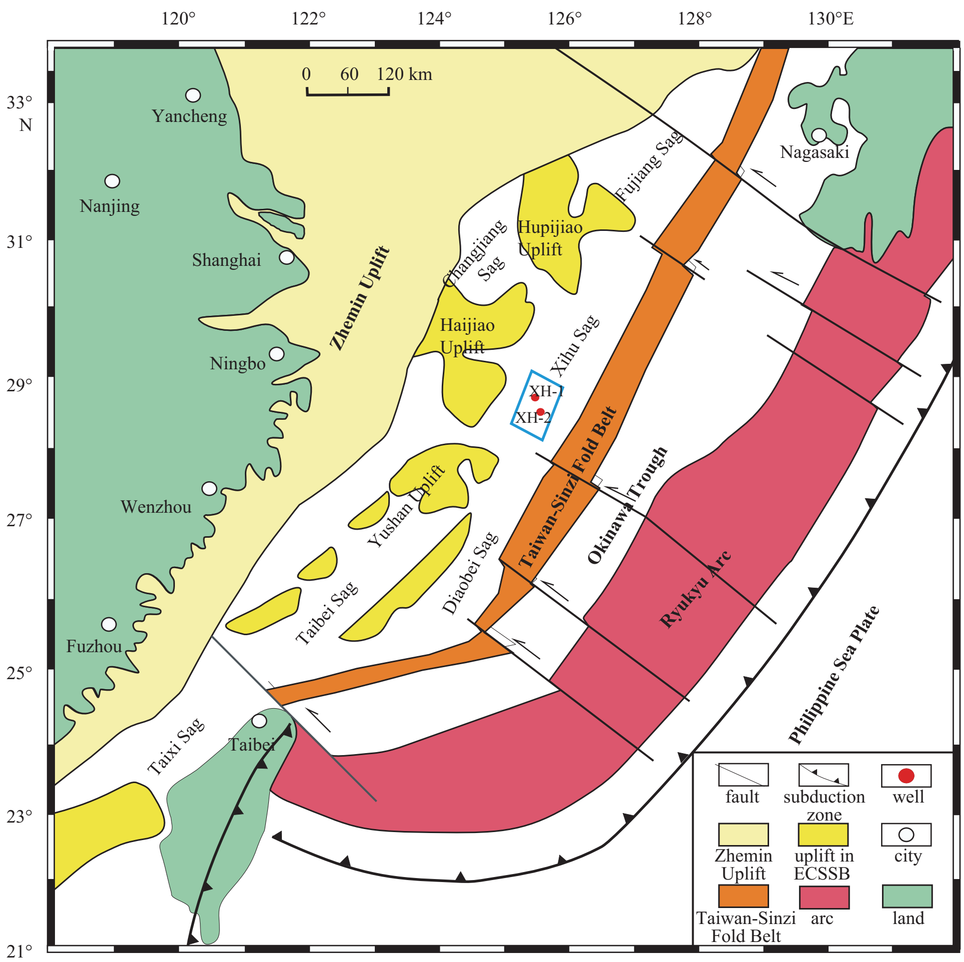

Fig. 1. Location map of the study area and tectonic framework of the East China Sea (modified after Wang, 1989).

proven to be the main reservoir for the oil and gas (Ye et al., 2008). Understanding diagenetic processes and cement sources in sandstones and their impact on reservoir quality are essential to further exploration, appraisal and production of hydrocarbon in the Xihu Sag, but only a few such studies for the Huagang Formation have been done so far (Ren et al., 1996; Pei, 2007; Zhang et al., 2009b; Hao et al., 2011). Furthermore, the timing of diagenesis and the origin of the cements, especially the diagenetic history and fluid evolution, have not been studied thoroughly. In this paper, using petrology, mineralogy and geochemistry (stable carbon and oxygen isotopes) approach to reconstruct the paleofluids evolution in the study area leading to the better prediction of hydrocarbon prospects within this area.

2 Geological background

The Eastern China Sea Shelf Basin, located within the convergence zone between the Eurasian, Pacific, and Philippine Sea Plates, contains thick sedimentary fills (exceeding 10 000 m in thickness) and abundant oil and gas resource (Zhou et al., 2002). The formation and evolution of the East China Sea Shelf Basin are closely related to the subduction of the Pacific Plate and the Philippine Sea Plate, and the collision between Indian Plate and Eurasian Plate (Xu and Zhang, 2000a, b ; Zang and Ning, 2002; Zhou et al., 2002). The Xihu Sag, covering 42 700 km^2, is located in the east of the East China Sea Shelf Basin and bounded to the west by the Haijiao Uplift, Hupijiao Uplift and Yushan Uplift, to the east by the Taiwan–Sinzi Fold Belt, to the south by the Diaobei Sag, and to the north by the Fujiang Sag (Fig. 1). It is a Mesozoice-Cenozoic shelf sedimentary basin which developed on Pre-Cambrian and Palaeozoic metamorphic basement.

Three stages of tectonic evolution were experienced in the Xihu Sag. First, an initial rifting stage showing fast subsidence rate occurred from the early Eocene to the end Eocene. The second is a thermal subsidence phase from the early Oligocene to the end of Miocene. From the Pliocene to present, a post-rift phase of the regional subsidence occurred throughout the East China Sea continental shelf (Zhong et al., 2001; Yang et al., 2004). The sedimentary sequence, with a maximum sediment thickness of more than 10 000 m, consists of eight formations (Baoshi, Pinghu, Huagang, Longjing, Yuquan, Liulang, Santan and Donghai Group) from bottom to top in the Xihu Sag (Fig. 2). From bottom to top, Baoshi oil and gas-bearing interval, Pinghu gas-bearing interval, Huagang and Longjing oil and gas-bearing intervals consist of the petroleum systems in the Xihu Sag. Economic oil and gas reservoirs are mostly distributed in Pinghu and Huagang intervals (Zhu et al., 2012). Hydrocarbon exploration has shown that at least 90% of the commercial reserves were found in the Pinghu Formation and Huagang Formation so far (Chen and Ge, 2003; Li and Li, 2003). The studied formation in this paper is the Huagang Formation of the Oligocene, which is an important hydrocarbon reservoir in the Xihu Sag. The Oligocene Huagang Formation has a thickness ranging from 1 000 to 2 000 m (Zhang et al., 2014). The Xihu Sag is given priority to with continental sedimentation, mainly by the lacustrine, fluvial and delta sedi-

System and series	Age /Ma	Formation	Depositional environment	Tectonic movement	Basin evolution
Quaternary		Donghai Group	shallow marine		regional subsidence
	2.59				
Pliocene		Santan	lacustrine	Longjing	
	5.33				
Miocene		Liulang	fluvial and lacustrine		depression
		Yuquan	fluvial and lacustrine		
		Longjing	shallow lacustrine lacustrine-delta	Huagang	
	23.03				
Oligocene		Huagang	fluvial and lacustrine	Yuquan	
	33.9				
Eocene		Pinghu	fluvial-delta		rifting and initial subsidence
		Baoshi	shallow marine	Oujiang	
	55.8				
Paleocene		absent	absent		uplift

Fig. 2. Filling sequences, sedimentation environment, and evolution of the Xihu Sag (modified from Chen and Ge, 2003; Yang et al., 2004).

mentary environment consisting of greywackes and shales alternating, interbedded with coal in Oligocene.

3 Samples and methods

Twenty-seven samples (thirteen sandstones, fourteen mudstones) of the Oligocene Huagang Formation clastic rocks were collected from key wells (XH-1, XH-2) in the south of Xihu Sag (Fig. 1). The lithology of sandstone samples is chiefly fine grained lithic quartz sandstone with medium-high texture maturity. The sandstones are characterized by medium sorted to well sorted, subrounded to rounded grains. The sandstone samples were vacuum impregnated with blue epoxy resin prior to thin section preparation which could assist the observation of pore types, feature, distribution and relationship with framework grains. The modal composition was obtained by counting 200-300 points in each thin section under polarization microscope with the photo-collecting system. Some samples were further observed under scanning electronic microscope (SEM).

Carbon and oxygen isotope composition of twenty samples were analyzed using a Thermo Finnigan MAT252 mass spectrometer at the Key Laboratory of Petroleum Resources Research, Institute of Geology and Geophysics, Chinese Academy of Sciences. The samples were crushed into 200 mesh powders by using a tungsten carbide steel pot. Minor amount of samples were reacted with 100% orthophosphate at a temperature of 90°C to obtain CO_2. Carbon and oxygen isotope compositions of samples were expressed with respect to the Peedee belemnite II standard (PDB II). Replicate measurements of the internal laboratory standard gave a total analytical precision of ±0.02‰ for both carbon and oxygen measurements.

4 Results and discussion

4.1 *Cements and indicating for fluids*

In general, cements are the most common in sediments, which supply information about the diagenetic history and the chemical composition of pore waters. The main cements in the Huagang Formation sandstones comprise chlorite, carbonate cements, quartz and kaolinite.

4.1.1 *Chlorite cement*

The origin of chlorite cement is complex and its precipitation is controlled by the pore water, material source, early clay minerals and sealing or opening of the system (Huang et al., 2004). It could develop from the stage of eodiagenesis to mesodiagenesis (Grigsby, 2001). The chlorite in the Huagang Formation sandstones occurs predominantly as the pore-lining cement. Pore-lining chlorites are present as coatings on framework grains particularly along the contacts between grain surfaces, including point contacts and line contacts (Figs 3a and b). This suggests that the pore-lining chlorites were precipitated before an initial phase of mechanical compaction in the burial history. Thus, this process typically occurred in eodiagenesis at a low temperature, which was most probably affected by the sedimentary environment not from the dissolution of feldspars, volcanic rock fragments and the alteration of clay minerals. These chlorites can be easily formed in a deltaic environment, especially in the deltaic front environment with abundant dissolved Mg and Fe ions from the weathering of volcanics and high pH value (Huang et al., 2004).

4.1.2 *Types of carbonate cements and their occurrences*

Carbonate cements are diagenetic minerals widespread in clastic rocks within different types of sedimentary basins (Abdel-Wahab and McBride, 2001; Rossi et al., 2001; Sun et al., 2002). Their formation history could involve the synsedimentary, early diagenetic and late diagenetic stages (Wang et al., 1999). Carbonate cements are very active in chemical properties, which are so

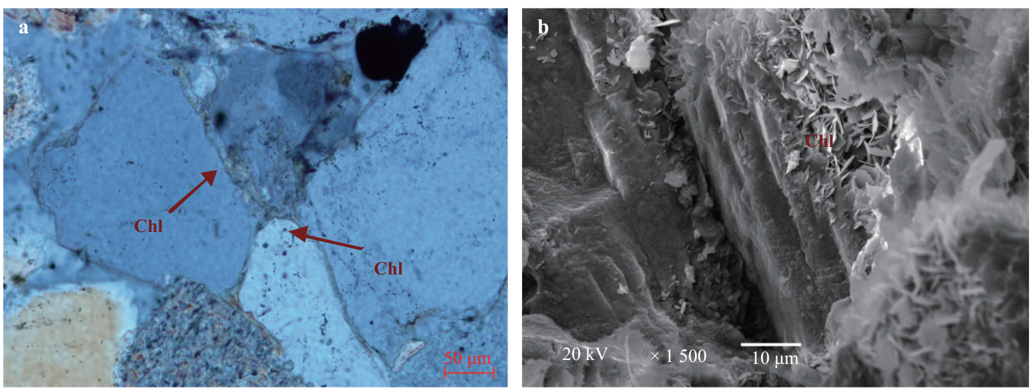

Fig. 3. Characteristics of chlorite cementation. a. Micrograph of thin section showing chlorite as coatings around detrital grains, XH-2, 3 035 m, feldspar quartz sandstone; and b. micrograph of SEM showing chlorite alone detrital grains, XH-2, 3 035 m, feldspar quartz sandstone. Chl indicates chlorite.

sensitive to the variation of acidity and alkalinity in pore fluid that they are easy to be dissolved and precipitated. Thus, multiple-phase carbonate cements could be used as the mineral indicator for the variation of fluid composition (Rossi et al., 2001; Wang et al., 1999).

Three types of carbonate cements, early siderite, medium ferrocalcite and late ankerite were identified through petrological and mineralogical observations. Early siderite fills in the primary intergranular pores (Fig. 4a), characterized by the dark crypto- to microcrystalline aggregation. Seldom replacing detrital grains and weak compaction indicate that the siderite was early precipitation. The siderite precipitation mainly produces in synsedimentary to early diagenetic stage depending on the weak acid, weak alkali to alkaline and highly activity of CO_2 environment (Zhu et al., 2008). Thus, the emergence of siderite shows that the original sedimentary environment presents a weak alkaline in the study area.

Medium ferrocalcite post-dates all the other diagenetic processes during mesodiagenesis, which is frequently present as a replacement mineral among detrital grains. In thin sections, ferrocalcite replaced quartz and precipitated in feldspar dissolution pores (Figs 4b and c), suggesting that ferrocalcite formed during late diagenesis after quartz cementation and feldspar dissolution.

Late ankerite usually shows clear and a clean crystal filling in the primary pore space (Fig. 4d), formed after quartz cementation and kaolinite precipitation, and seldom replaces detrital grains. This type of cement usually has dual impact on clastic reservoir properties. On the one hand, scattered carbonate cements could improve the anti-compaction ability of sandstones and keep higher intergranular volume, which could provide the mass basis for the later dissolution. On the other hand, higher carbonate cements would block pore throat and then reduce reservoir physical properties.

4.1.3 *Oxygen and carbon isotopic compositions of carbonate cements*

The carbon and oxygen isotopic compositions of carbonate cements could be used to identify the geochemical environment and material source during their formation (Rosenbaum and Sheppard, 1986; Huang et al., 2002; McBride and Parea, 2001; Wang et al., 2007, 2010; Dong et al., 2004; Zhu et al., 2007). The carbon isotope could constrain the carbon source in diagenetic fluids (Macaulay et al., 1993; Fayek et al., 2001), and the oxygen isotopic composition of carbonate cements could be used to estimate the temperature during their precipitation. Generally, $\delta^{18}O$ of carbonate cements becomes lighter with their increased formation temperature. To distinguish the formation environment (freshwater and marine), Keith and Weber (1964) proposed an empirical formula, as follows:

$$Z = 2.048\times\left(\delta^{13}C+50\right)+0.498\times\left(\delta^{18}O+50\right), \qquad (1)$$

where $\delta^{13}C$ and $\delta^{18}O$ values follow the PDB standard. Z can be used to indicate ancient salinity (Keith and Weber, 1964; Zhang, 1985), Z<120 indicates freshwater, and Z>120 indicates marine. The Z values of the sandstones in this area are 108.8 to 114.9 with an average of 112.4, which are all less than 120, indicating that

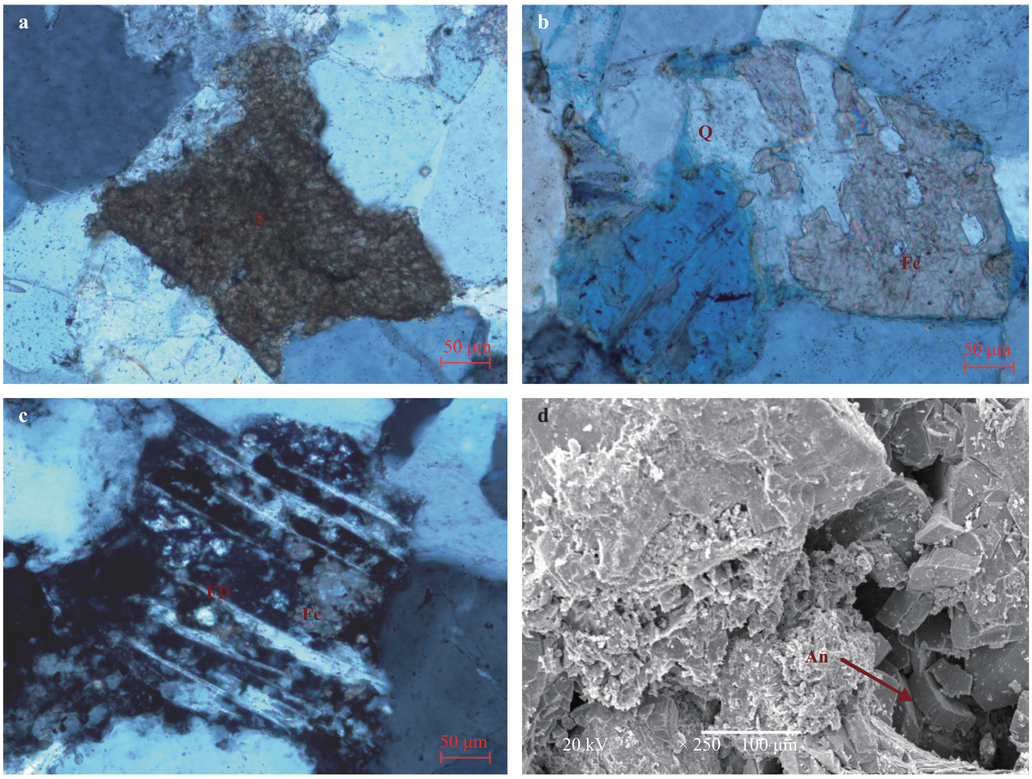

Fig. 4. Characteristics of carbonate cementation. a. Micrograph of thin section showing early siderite filling primary intergranular pore, XH-1, 3 196.25 m, lithic quartz sandstone; b. micrograph of thin section showing ferrocalcite replacing quartz, XH-2, 3 850.45 m, lithic quartz sandstone; c. micrograph of thin section showing ferrocalcite filling feldspar dissolution pore, XH-1, 3 610.5 m, lithic quartz sandstone; d. micrograph of SEM showing ankerite filling pore, XH-1, 3 606.73 m, lithic quartz sandstone. S indicates siderite, Q detrital quartz, FD feldspar dissolution, Fc ferrocalcite, and An ankerite.

the diagenetic fluids of carbonate cements are mainly freshwater. The Z values of mudstones range from 103.7 to 123.0 (mean= 114.6), which indicate that the origin of the pore water is mainly freshwater with a slight mixed of saltwater.

The mudstone samples are relatively concentrated in oxygen isotopic composition ranging from –8.1‰ to –13.5‰ (mean= –11.2‰), whereas $\delta^{13}C$ varying over a wide range from –8.7‰ to 1.0‰ (mean=–3.6‰), implying that carbonate minerals have the similar formed temperature but from different diagenetic fluids. According to the $\delta^{13}C$ values, the mudstone samples can be separated into two groups. The $\delta^{13}C$ values for Groups I and II are –2.5‰ to 1‰ and –8.7‰ to –3.7‰, respectively (Fig. 5). Due to the $\delta^{13}C$ values of lacustrine carbonate ranges between –2‰ and 6‰ (Kelts and Talbot, 1990), so the carbonate of Group I samples should precipitate from lacustrine environment. The $\delta^{13}C$ values of Group II samples are lighter than Group I samples, but the $\delta^{18}O$ values are approximately the same with Group I. It suggests that the two carbonate mineral groups have nearly same low formed temperature and the shallow buried depth. The $\delta^{13}C$ value of CO_2 dissolved in meteoric water is –7‰ (Wang et al., 2010), and the carbon isotope of CO_2 generated by thermal decarboxylation of organic material with high temperature is ranging from –4.0‰ to –35.0‰ (Suess and Whiticar, 1989). Considering the low $\delta^{18}O$ values, the formation of carbonate minerals of Group II samples have little relationship with decarboxylation, but are closely related to the meteoric water leaching due to the Huagang Formation uplifting.

The carbon and oxygen isotopic values of the sandstone samples are –4.4‰ to –2.3‰ and –14.3‰ to –19.1‰, respectively. The $\delta^{13}C$ and $\delta^{18}O$ values of some samples are close to Group I mudstones (Fig. 5), implying that the formation environment of carbonate cements are alkaline lake similar with Group I mudstones. However, the other samples have relatively light $\delta^{13}C$ values similar with Group II mudstones, but $\delta^{18}O$ values are lighter than Group II mudstones suggesting that the carbonate cements formation temperature of the sandstone samples are higher than Group II mudstones. With increasing temperature due to increased burial depth, CO_2 with lighter carbon isotope ($\delta^{13}C$ values ranging from –4.0‰ to –35.0‰) is generated by thermal decarboxylation of organic material. Considering the high formation temperature, the carbonate cements formation of sand samples with lighter $\delta^{13}C$ values should relate to the decarboxylation not the meteoric water leaching. When organic acid and CO_2 entered the sandstone reservoir, the feldspar, lithic fragments and early carbonate cements were dissolved to form secondary pores and generate authigenic quartz and kaolinite. During peak generation of source rocks, a large number of hydrocarbon infilling the sandstone reservoir would make the acidic environment transform to alkaline environment. Under the alkaline condition, CO_2 dissolved in pore water easily combined with Ca and Fe ions forming ferriferous calcite to replace authigenic quartz or precipitate in secondary pores formed in acidic environment.

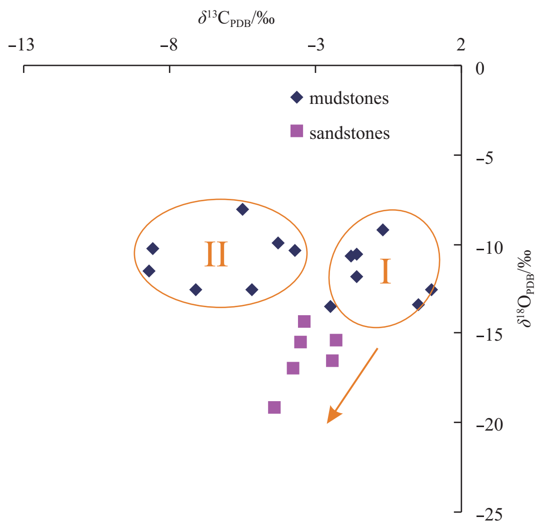

Fig. 5. $\delta^{13}C_{PDB}$ vs. $\delta^{18}O_{PDB}$ diagram.

4.1.4 *Quartz cement*

Quartz cement is generally common cements in the study area. Authigenic quartz in the sandstones occurs mainly as partial to complete syntaxial overgrowths (10–60 μm thick) around quartz grains (Figs 6a and b), which are easy to discriminate from the quartz grains due to the existence of some dust rims. In SEM samples, small quartz crystals filling the intergranular or secondary intragranular space can be identified (Fig. 6c), which are difficult to distinguish from detrital quartz grains by the polarizing microscope. In addition, authigenic quartz is always found together with kaolinite (Fig. 6b). The authigenic quartz often occupies primary pores, significantly reducing the porosity and blocking narrow pore-throats.

The Pinghu and Huagang Formations include organic-rich mudstones, shales and coals which occur widely at depths greater than 2 300 m. Most of these potential source rocks have entered the oil window (Chen and Ge, 2003). CO_2 and organic acids were generated at 80–120°C in the thermal evolution of the organic matters (Surdam et al., 1989). The acidic fluids were expelled into sandstones from source rocks by compaction and overpressure related to hydrocarbon generation and clay dehydration. When organic acid and CO_2 filled in the sandstone reservoir, the feldspar, lithic fragments and carbonate cements were dissolved. If concentrations of Al^{3+} and SiO_2 (aq) in pore waters exceed the concentrations needed for saturation of kaolinite and quartz, the dissolution and precipitation will occur. The reactions can be expressed by the following equation (Giles and de Boer, 1990):

$$KAlSi_3O_8 + H^+ + 0.5H_2O = 0.5Al_2Si_2O_5(OH)_4 + 2SiO_2 + K^+, \quad (2)$$

where $KAlSi_3O_8$ is K-feldspar, $Al_2Si_2O_5(OH)_4$ is kaolinite and SiO_2 is quartz. In addition, silica released from local dissolution of quartz or mica is possibly another supply (Walker, 1960; McBride, 1989).

4.1.5 *Kaolinite cement*

Kaolinite cement is mainly present as euhedral booklets and vermicular aggregates filling primary pores as well as within secondary pores in feldspar grains (Fig. 6d). Kaolinite occurs as stacks of pseudo hexagonal plates or books. Kaolinite cement generally derives from the dissolution of feldspars, lithic fragments and biotites by acid fluids during mesodiagenesis, and is always accompanied by minor amounts of microcrystalline authigenic quartz (Fig. 6b). Thus, kaolinite can be used as the indicator mineral for the acid fluid.

4.2 *Dissolution*

The investigated sandstone samples experienced two main episodes of dissolution during diagenesis. Petrographic examina-

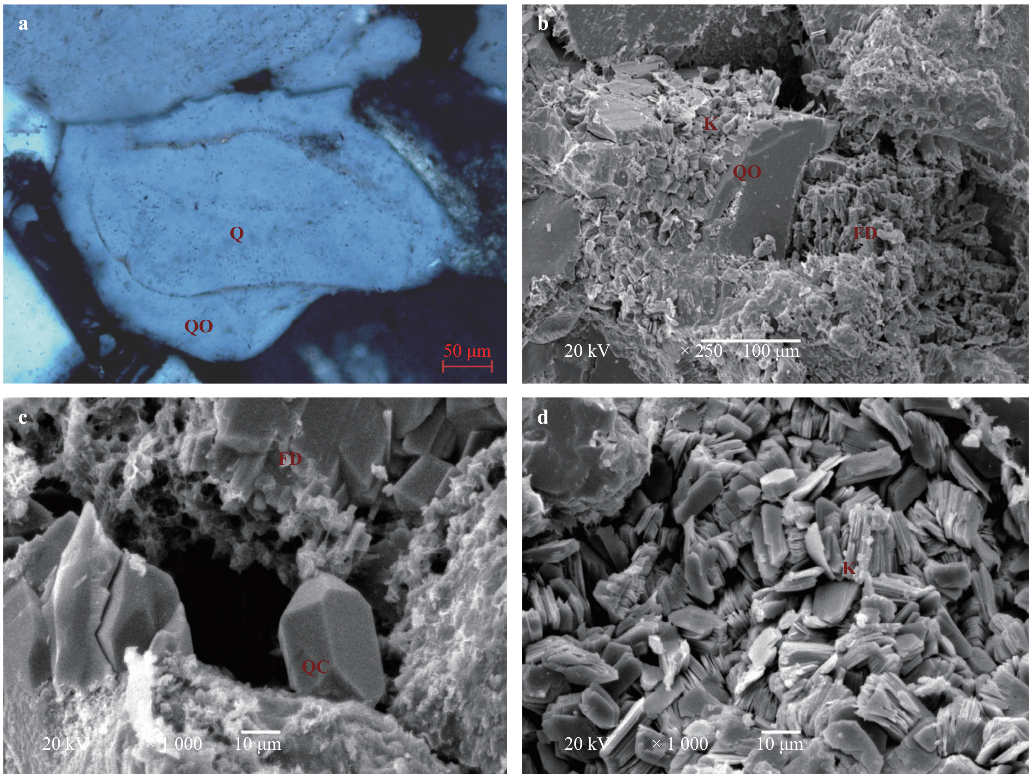

Fig. 6. Characteristics of quartz and kaolinite cementation. a. Micrograph of thin section showing quartz overgrowth, XH-1, 3 610.5 m, lithic quartz sandstone; b. micrograph of SEM showing feldspar dissolution, authigenic kaolinite and quartz cement, XH-1, 3 606.73 m, lithic quartz sandstone; c. micrograph of SEM showing quartz crystal filling pore, XH-1, 3 606.73 m, lithic quartz sandstone; and d. micrograph of SEM showing authigenic kaolinite aggregates filling pore, XH-1, 3 107.5 m, lithic quartz sandstone. Q indicates detrital quartz, QO quartz overgrowth, QC quartz crystal, FD feldspar dissolution, and K kaolinite.

tions suggest that unstable components such as feldspar, lithic fragments, and carbonate cement are dissolved support a scenario of early dissolution by organic acid which was produced by thermal decarboxylation of organic material (Brown et al., 1989; Taylor et al., 2000; Dutton, 2008). Feldspar grains and lithic fragments encountered partial to complete dissolution making a large amount of secondary pores in such process (Figs 7a and b). In addition, this dissolution could produce authigenic quartz or overgrowth and kaolinite during this period. The second episode of dissolution occurred in the alkaline conditions. When the pH value of the pore water is higher than 7, the quartz and other silicate minerals tend to be unstable and are dissolved in burial environments with high temperature, high pressure and ionic concentration. In the thin sections, the quartz grains are characterized by corroded boundaries, irregular pitted and embayment margins (Fig. 7c), even exhibit dissolution textures replaced with poikilotopic calcite precipitation (Fig. 4b). Under alkaline conditions, it is suitable for calcite precipitation (Epstein and Freidman, 1982; Zaid and Al Gahtani, 2015).

4.3 *Oil presence characteristics*

Two oil phases were identified based on the thin section and fluorescence observations. The fluorescence colors of two oil phases are primarily yellow-green and blue (Fig. 7d), respectively. The colors of the oil indicated that the oil is relative low mature and light (Zhang et al., 2009a; Dong et al., 2014). In addition, the homogenization temperatures of fluid inclusions also show that two main phases of hydrocarbon charging occurred at the end of the Miocene and in the Quaternary, respectively (Su, 2014).

4.4 *Typical diagenetic parasequences*

Although it is difficult to obtain precise timing and duration of the diagenetic processes, the relative timing of the primary diagenetic features in the Huagang Formation sandstones in the south Xihu Sag was reconstructed based on textural relationships from thin sections and SEM examinations. In summary, the dominant eogenetic features in the sandstones of the Huagang Formation are the formation of thin authigenic clay coatings around the detrital grains and the precipitation of early carbonate cement. Subsequent mesogenetic changes experienced by these sandstones including compaction, dissolution of feldspars and lithic fragments, development of quartz overgrowths, ferrocalcite cementation, and pore-filling kaolinite and so on. The diagenetic parasequences of the Huagang Formation sandstones could be summarized as follows: early calcite precipitation→mechanical compaction→influx of fluid flow with organic acids→dissolution of feldspar and lithic fragments→secondary porosity→authigenic kaolinite + authigenic quartz→hydrocarbon emplacement→medium ferrocalcite filling the primary and secondary pores→dissolution of quartz and other silicate minerals→late ankerite filling→hydrocarbon emplacement (Fig. 8). According to the petroleum and natural gas industry standards of the People's Republic of China (SY/T 5477-2003: the division of diagenetic stages in clastic rocks), it is believed that most of the Huagang Formation sandstones are now in Period B of the mesodiagenesis.

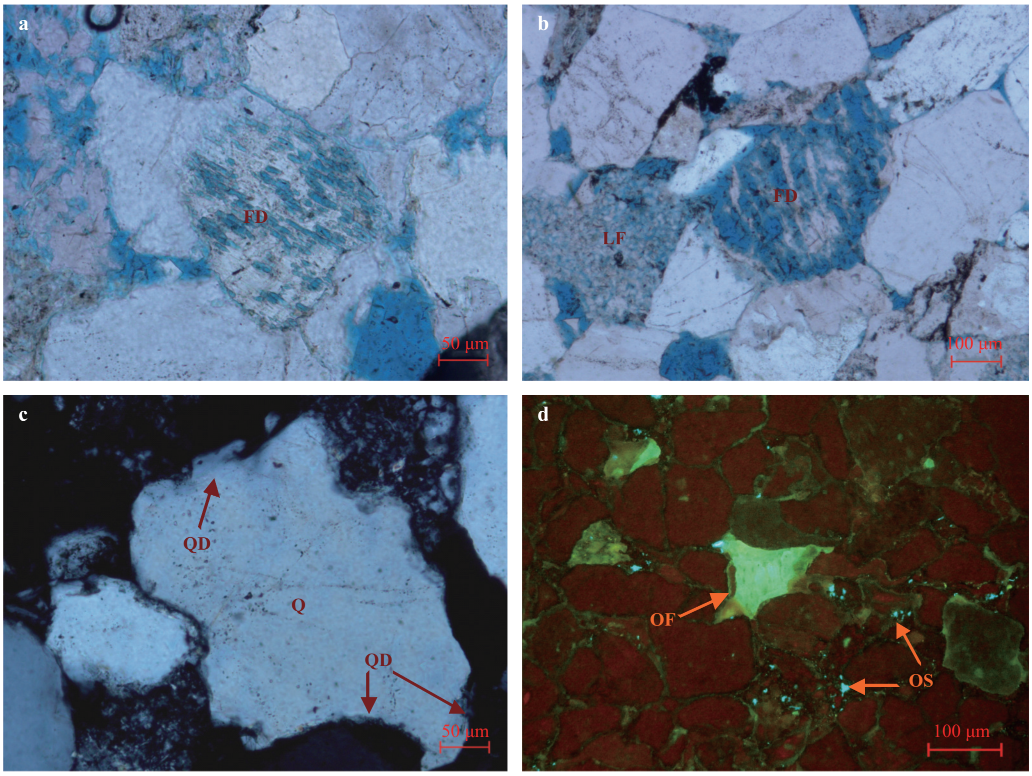

Fig. 7. Characteristics of dissolution and oil presence forms from fluorescence observation. a. Micrograph of thin section showing feldspar dissolved along the cleavage, XH-2, 3 852.95 m, lithic sandstone; b. micrograph of thin section showing the dissolution of feldspar and lithic fragment, XH-1, 3 608.2 m, lithic quartz sandstone; c. micrograph of thin section showing quartz dissolution, XH-1, 2 789.25 m, lithic sandstone; and d. fluorescence observation showing first oil with yellow-green color and second oil with blue color, XH-1, 3 610.5 m, lithic quartz sandstone. Q indicates detrital quartz, QD quartz dissolution, FD feldspar dissolution, LF lithic fragment, OF first oil with yellow-green color, and OS second oil with blue color.

4.5 *Fluids evolution and interaction with rocks*

During the eodaigenetic stage, the burial depth was less than 1 500 m, the Ro values were less than 0.5%, and the percentage of smectite layers exceeded 50% in the I/S (Fig. 8). Mechanical compaction and early calcite cementation were the predominant diagenetic processes at shallow depths. Eodiagenesis included all processes that occurred at or near the surface of the sediments, where the chemistry of the interstitial water was controlled mainly by the depositional environment (Choquette and Pray, 1970). The Xihu Sag was mainly the lacustrine and delta sedimentary environment in Oligocene. The δ^{13}C values of Group I samples show that the early calcite precipitates from alkaline lacustrine environment with oversaturated carbonate calcium. In addition, the *Z* values of samples are near 120, indicating that the origin sedimentary water is mainly freshwater with a slight mixed of saltwater. That is, the lake suffered transgression during the deposition in Oligocene. Under the alkaline lacustrine environment, the deltaic front environments with sufficient dissolved Mg and Fe ions from the weathering of volcanics formed chlorites along detrital grains. With increasing burial depth, the detrital grains including quartz and feldspars were rearranged, and the ductile mud fragments were transformed to pseudomatrix due to compaction. The Hugang Event occurred in the late Oligocene, resulting in local uplift and erosion of the Huagang Formation (Fig. 8). The tectonic uplift promoted leaching by meteoric water but it had little effect on the Huagang Formation reservoir from the evidence of the light δ^{13}C values in the carbonate cements of sandstones.

The Xihu Sag subsidence recommenced after the Oligocene resulted in re-compaction leading to porosity reduction. At the early of the Miocene, the most of Huagang Formation entered the mesodaigenetic stage. During this stage, the burial depth were from 1 500 m to 4 000 m (Fig. 8), the Ro values ranged from 0.5% to 2.0%, and the smectite content decreased from 50% to less 15% in the I/S. With increasing burial depth, the temperature and pressure gradually increased to boost decarboxylation of organic matter in source rocks and generated part of CO_2 and organic acids with lighter carbon isotope. Trough compaction and overpressure, the acidic fluids entered into sandstones along fault from source rocks. Then the feldspar, lithic fragments and carbonate cements were dissolved and generated secondary pores, authigenic kaolinite and quartz. At the end of the Miocene, the Longjing Event occurred, which was the most intensive tectonic movement in the Xihu Sag, resulting that a large number of hydrocarbon migrated into the sandstone reservoir from the source rock. After the hydrocarbon entered the reservoir, the intensive of the dissolution and cementation were slowed down, but also occurred the dissolution of the quartz and the precipitation of the carbonate cement under the alkaline condition. The last hydrocarbon charging occurred in the Quaternary, after most of the sandstones became tight reservoirs.

5 Conclusions

The Huagang Formation sandstone reservoir has experienced significant early and medium diagenetic processes. The early diagenetic processes included the chlorite coating around

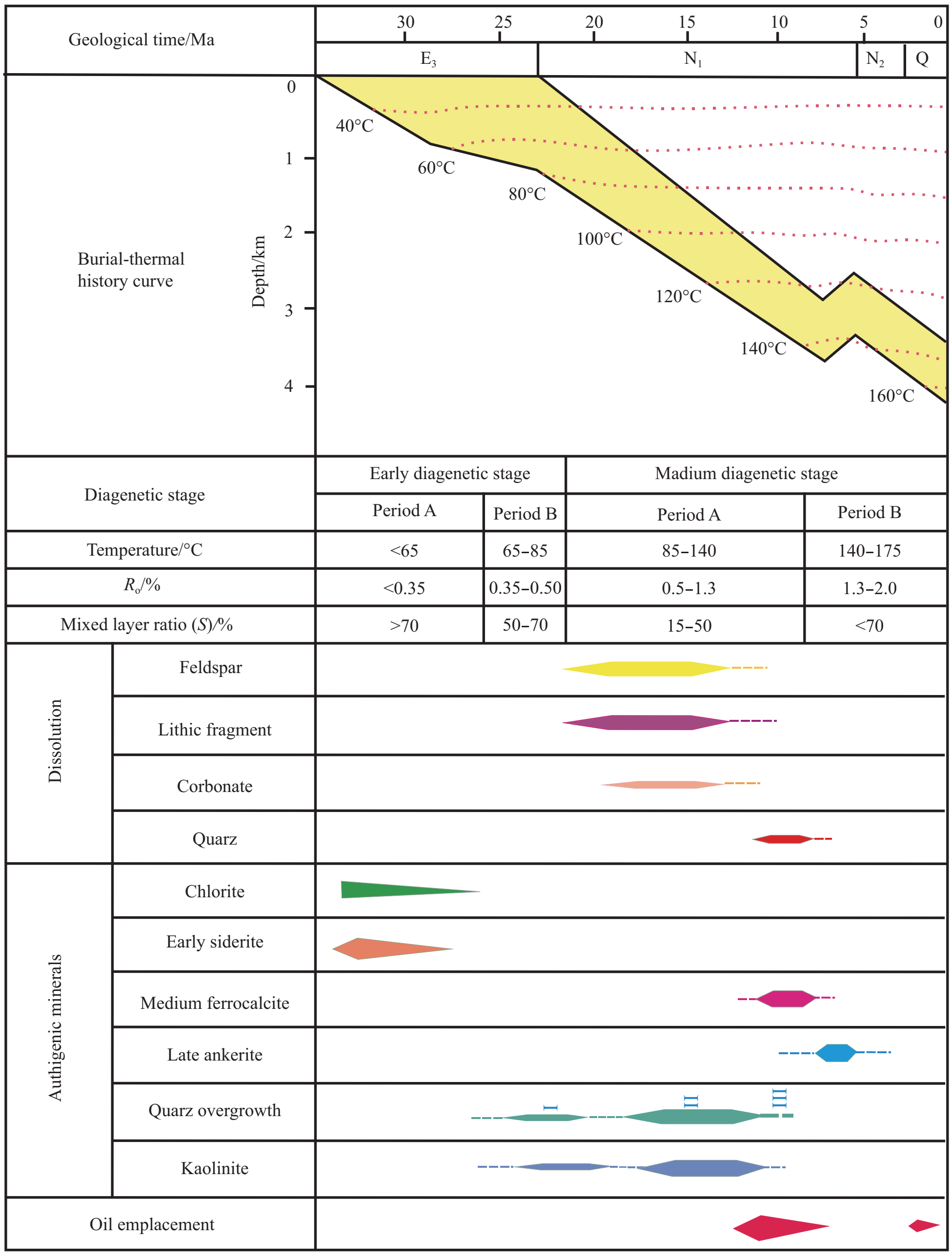

Fig. 8. Burial-thermal history and typical paragenetic sequences.

the detrital grains and the precipitation of early carbonate cement. Deep burial medium diagenetic processes included dissolution of feldspars and lithic fragments, development of quartz overgrowths, pore-filling kaolinite, ferrocalcite cementation, and quartz dissolution and so on. The oxygen and carbon isotopic compositions of carbonate cements indicate that the origin of the pore water was main freshwater with a slight mixed of saltwater. The Huagang Formation sandstone reservoir experienced two dissolutions during diagenesis. The early dissolution is that the organic acidic water dissolved unstable components such as feldspar, lithic fragments, and carbonate cement. The second dissolution is that quartz and other silicate minerals were dissolved under the alkaline condition. Two main phases of hydrocarbon charging occurred at the end of the Miocene and in the Quaternary period, respectively. The first hydrocarbon charging occurred posterior to feldspar dissolution and the second hydrocarbon charging occurred after the late carbonate precipitation.

References

Abdel-Wahab A, McBride E F. 2001. Origin of giant calcite-cemented concretions, temple member, Qasr El Sagha formation (Eocene), Faiyum depression, egypt. Journal of Sedimentary Research, 71(1): 70–81

Brown D M, McAlpine K D, Yole R W. 1989. Sedimentology and sandstone diagenesis of Hibernia Formation in Hibernia oil field, Grand Banks of Newfoundland. AAPG Bulletin, 73(5): 557–575

Chen Zhiyong, Ge Heping. 2003. Inversion structures and hydrocarbon accumulation in Xihu Sag, East China Sea Basin. China Offshore Oil and Gas (Geology) (in Chinese), 17(1): 20–24

Choquette P W, Pray L C. 1970. Geologic nomenclature and classification of porosity in sedimentary carbonates. AAPG Bulletin, 54(2): 207–250

Dong Tian, He Sheng, Wang Dexi, et al. 2014. Hydrocarbon migration and accumulation in the Upper Cretaceous Qingshankou Formation, Changling Sag, southern Songliao Basin: insights from integrated analyses of fluid inclusion, oil source correlation and basin modelling. Journal of Asian Earth Sciences, 90: 77–87

Dong Fuxiang, Liu Li, Ma Yanping. 2004. Carbon and oxygen isotopes of calcite cement in the lower part of the Sha-1 Formation, the Dagang beach area. Petroleum Geology & Experiment (in Chinese), 26(6): 590–593

Dutton S P. 2008. Calcite cement in Permian deep-water sandstones, Delaware Basin, west Texas: origin, distribution, and effect on reservoir properties. AAPG Bulletin, 92(6): 765–787

Epstein S A, Friedman G M. 1982. Processes controlling precipitation of carbonate cement and dissolution of silica in reef and near-reef settings. Sedimentary Geology, 33(3): 157–171

Fayek M, Harrison T M, Grove M, et al. 2001. *In situ* stable isotopic evidence for protracted and complex carbonate cementation in a petroleum reservoir, North Coles Levee, San Joaquin Basin, California, U.S.A. Journal of Sedimentary Research, 71(3): 444–458

Gier S, Worden R H, Johns W D, et al. 2008. Diagenesis and reservoir quality of Miocene sandstones in the Vienna Basin, Austria. Marine and Petroleum Geology, 25(8): 681–695

Giles M R, de Boer R B. 1990. Origin and significance of redistributional secondary porosity. Marine and Petroleum Geology, 7(4): 378–397

Grigsby J D. 2001. Origin and growth mechanism of authigenic chlorite in sandstones of the lower Vicksburg Formation, South Texas. Journal of Sedimentary Research, 71(1): 27–36

Hao Lewei, Liu Chang, Wang Qi, et al. 2011. Provenance characteristics of Huagang formation (Paleogene) in Xihu sag, East China Sea. Natural Gas Geoscience, 22(2): 315–323

Hsu S K, Sibuet J C, Shyu C T. 2001. Magnetic inversion in the East China Sea and Okinawa Trough: Tectonic implications. Tectonophysics, 333(1-2): 111–122

Huang Sijing, Shi He, Zhang Meng, et al. 2002. Application of strontium isotope stratigraphy to diagenesis research. Acta Sedimentologica Sinica (in Chinese), 20(3): 359–366

Huang Sijing, Xie Lianwen, Zhang Meng, et al. 2004. Formation mechanism of authigenic chlorite and relation to preservation of porosity in nonmarine Triassic reservoir sandstones, Ordos Basin and Sichuan Basin, China. Journal of Chengdu University of Technology (Science & Technology Edition) (in Chinese), 31(3): 273–281

Hunt J M. 1990. Generation and migration of petroleum from abnormally pressured fluid compartments. AAPG Bulletin, 74(1): 1–12

Keith M L, Weber J N. 1964. Isotopic composition and environmental classification of selected limestones and fossils. Geochimica et Cosmochimica Acta, 28(10-11): 1787–1816

Kelts K, Talbot M. 1990. Lacustrine carbonates as geochemical archives of environmental change and biotic/abiotic interactions. In: Tilzer M M, Serruya C, eds. Large Lakes. Berlin Heidelberg: Springer, 288–315

Li Shangqing, Li Chunjie. 2003. Analysis on the petroleum resource distribution and exploration potential of the Xihu Depression, the East China Sea. Petroleum Geology & Experiment (in Chinese), 25(6): 721–728

Macaulay C I, Haszeldine R S, Fallick A E. 1993. Distribution, chemistry, isotopic composition and origin of diagenetic carbonates; Magnus sandstone, North Sea. Journal of Sedimentary Research, 63(1): 33–43

McBride E F. 1989. Quartz cement in sandstones: a review. Earth-Science Reviews, 26(1-3): 69–112

McBride E F, Parea G C. 2001. Origin of highly elongate, calcite-cemented concretions in some Italian coastal beach and dune sands. Journal of Sedimentary Research, 71(1): 82–87

Mu Shuguang, Zhang Yiming. 1994. Reservoirs pores evolution under the control of diagenesis and stage. Journal of Southwest Petroleum Institute (in Chinese), 16(3): 22–27

Osborne M J, Swarbrick R E. 1999. Diagenesis in North Sea HPHT clastic reservoirs-consequences for porosity and overpressure prediction. Marine and Petroleum Geology, 16(4): 337–353

Pei Changrong. 2007. Authigenic carbonate mineral in the early tertiary sandstone of south central Xihu depression [dissertation] (in Chinese). Chengdu: Chengdu University of Technology

Qiu Longwei, Jiang Zaixing. 2006. Alkaline Diagenesis of Terrigenous Clastic Rocks (in Chinese). Beijing: Geological Publishing House, 1–2

Ren Zhengping, Bao Zhu, Qian Jianzhong. 1996. Features and controlling factors of sandstone reservoir in the south part of the Xihu depression. Marine Geology & Quaternary Geology (in Chinese), 16(1): 69–76

Rosenbaum J, Sheppard S M F. 1986. An isotopic study of siderites, dolomites and ankerites at high temperature. Geochimica et Cosmochimica Acta, 50(6): 1147–1150

Rossi C, Marfil R, Ramseyer K, et al. 2001. Facies-related diagenesis and multiphase Siderite cementation and dissolution in the reservoir sandstones of the Khatatba Formation, Egypt's Western Desert. Journal of Sedimentary Research, 71(3): 459–472

Stroker T M, Harris N B, Elliott W C, et al. 2013. Diagenesis of a tight gas sand reservoir: upper Cretaceous Mesaverde Group, Piceance Basin, Colorado. Marine and Petroleum Geology, 40: 48–68

Su Ao. 2014. Controlling factors of oil and gas accumulation of central inversion tectonic belt in Xihu depression, east China sea basin [dissertation]. Wuhan: China University of Geosciences

Suess E, Whiticar M J. 1989. Methane-derived CO_2 in pore fluids expelled from the Oregon subduction zone. Palaeogeography, Palaeoclimatology, Palaeoecology, 71(1-2): 119–136

Sun Yushan, Shen Yinmin, Xu Xun, et al. 2002. Properties by the analysis technique of the diagenetic lithofacies-taking Hadexun area in Tarim basin as an example. Acta Sedimentologica Sinica (in Chinese), 20(1): 55–60

Surdam R C, Crossey L J, Hagen E S, et al. 1989. Organic-inorganic interactions and sandstone diagenesis. AAPG Bulletin, 73(1): 1–23

Taylor K G, Gawthorpe R L, Curtis C D, et al. 2000. Carbonate cementation in a sequence-stratigraphic framework: upper Cretaceous sandstones, Book Cliffs, Utah-Colorado. Journal of Sedimentary Research, 70(2): 360–372

Taylor T R, Giles M R, Hathon L A, et al. 2010. Sandstone diagenesis and reservoir quality prediction: models, myths, and reality. AAPG Bulletin, 94(8): 1093–1132

Walker T R. 1960. Carbonate replacement of detrital crystalline silicate minerals as a source of authigenic silica in sedimentary rocks. Geological Society of America Bulletin, 71(2): 145–152

Wang Guochun. 1989. Positive inverted structures in southwest of the East China Sea Basin. Oil & Gas Geology (in Chinese), 10(2): 137–144

Wang Qi, Hao Lewei, Chen GuoJun, et al. 2010. Forming mechanism of carbonate cements in siliciclastic sandstone of Zhuhai Formation in Baiyun sag. Acta Petrolei Sinica (in Chinese), 31(4): 553–558

Wang Qi, Shi Ji'an, Xue Lianhua, et al. 1999. Characteristics of fluid-rock interaction in clastic reservoir controlled by evolution of diagenetic environment-taking the southwest depression of Tarim basin as an example. Acta Sedimentologica Sinica (in Chinese), 17(4): 584–590

Wang Qi, Zhuo Xizhun, Chen Guojun, et al. 2007. Characteristics of carbon and oxygen isotopic compositions of carbonate cements in Triassic Yanchang sandstone in Ordos Basin. Natural Gas Industry (in Chinese), 27(10): 28–32

Wilkinson M, Darby D, Haszeldine R S, et al. 1997. Secondary porosity generation during deep burial associated with overpressure leak-off: fulmar Formation, United Kingdom Central Graben. AAPG Bulletin, 81(5): 803–813

Xu Junyuan, Zhang Lingyun. 2000a. Genesis of Cenozoic basins in northwest Paci?c Margin (2): linked dextral pull-apart basin system Oil & Gas Geology (in Chinese), 21(3): 185–190

Xu Junyuan, Zhang Lingyun. 2000b. Genesis of Cenozoic basins in northwest Paci?c Margin (3): tectonic evolution of post rifting period Oil & Gas Geology (in Chinese), 21(3): 287–292

Yang Shuchun, Hua Shengbiao, Cai Dongsheng, et al. 2004. Present-day heat flow, thermal history and tectonic subsidence of the East China Sea Basin. Marine and Petroleum Geology, 21(9): 1095–1105

Ye Jiaren, Gu Huirong, Jia Jianyi. 2008. Petroleum geological condition and exploration potential of Xihu depression, East China Sea. Marine Geology & Quaternary Geology (in Chinese), 28(4): 111–116

Zaid S M, Al Gahtani F. 2015. Provenance, diagenesis, tectonic setting, and geochemistry of Hawkesbury Sandstone (Middle Triassic), southern Sydney Basin, Australia. Turkish Journal of Earth Sciences, 24: 72–98

Zang Shaoxian, Ning Jieyuan. 2002. Interaction between Philippine Sea plate (PH) and Eurasia (EU) plate and its influence on the movement Eastern Asia. Chinese Journal of Geophysics (in Chinese), 45(2): 188–197

Zhang Xiulian. 1985. Relationship between carbon and oxygen stable isotope in carbonate rocks and paleosalinity and paleotemperature of seawater. Acta Sedimentologica Sinica (in Chinese), 3(4): 17–30

Zhang Liuping, Bai Guoping, Luo Xiaorong, et al. 2009a. Diagenetic history of tight sandstones and gas entrapment in the Yulin Gas Field in the central area of the Ordos Basin, China. Marine and Petroleum Geology, 26(6): 974–989

Zhang Jianpei, Ge Heping, Qi Binwen. 2009b. Characteristics of authigenic kaolinite in sandstones of Xihu Sag and it's impact on reservoir physical properties. Offshore Oil (in Chinese), 29(1): 1–8

Zhang Hu, Guo Yinghai, Zhao Zhigang, et al. 2014. Study on seam features and control factors of Huagang formation of Xihu depression in east sea. Coal Science and Technology (in Chinese), 42(11): 97–100

Zhang Xia, Lin Chunming, Cai Yuanfeng, et al. 2012. Pore-lining chlorite cements in lacustrine-deltaic sandstones from the upper Triassic Yanchang Formation, Ordos Basin, China. Journal of Petroleum Geology, 35(3): 273–290

Zhong Dalai, Ding Lin, Ji Jianqing, et al. 2001. Coupling of the lithospheric convergence of west China and dispersion of east China in Cenozoic: link with paleoenvironmental changes. Quaternary Sciences (in Chinese), 21(4): 303–312

Zhou Zuyi, Jia Jianyi, Li Jiabiao, et al. 2002. Quantitative study on inversion structures in Xihu Depression, East China Sea: constraints from fission track analysis data. Marine Geology & Quaternary Geology (in Chinese), 22(1): 63–67

Zhu Yangming, Li Ying, Zhou Jie, et al. 2012. Geochemical characteristics of tertiary coal-bearing source rocks in Xihu depression, east China sea basin. Marine and Petroleum Geology, 35(1): 154–165

Zhu Yangming, Zheng Xia, Liu Xinshe, et al. 2007. Stable carbon isotope of authigenetic calcite used in reservoirs to tracing the hydrocarbon migration. Natural Gas Industry (in Chinese), 27(9): 24–27

Zhu Rukai, Zou Caineng, Zhang Nai, et al. 2008. Diagenetic fluids evolution and genetic mechanism of tight sandstone gas reservoirs in Upper Triassic Xujiahe Formation in Sichuan Basin, China. Science in China Series D: Earth Sciences, 51(9): 1340–1353